

Hawking-like emission in kink-soliton escape from a potential well

J A González^{1,2}, M A García-Ñustes¹, A Sánchez³
and P V E McClintock²

¹ Centro de Física, Instituto Venezolano de Investigaciones Científicas (IVIC), A.P. 21827, Caracas 1020-A, Venezuela

² Department of Physics, Lancaster University, Lancaster LA1 4YB, UK

³ Grupo Interdisciplinar de Sistemas Complejos (GISC), Departamento de Matemáticas, Universidad Carlos III de Madrid, 28911 Leganés, Madrid, Spain
E-mail: jorge@ivic.ve, mogarcia@ivic.ve, p.v.e.mcclintock@lancaster.ac.uk
and anxo@math.uc3m.es

New Journal of Physics **10** (2008) 113015 (19pp)

Received 16 July 2008

Published 11 November 2008

Online at <http://www.njp.org/>

doi:10.1088/1367-2630/10/11/113015

Abstract. The escape of solitons over a potential barrier is analysed within the framework of a nonlinear Klein–Gordon equation. It is shown that the creation of a kink–antikink pair near the barrier through an internal mode instability can be followed by escape of the kink in a process analogous to Hawking radiation. These results have important implications in a wider context, including stochastic resonance and ratchet systems, which are also discussed.

Contents

| | |
|---|-----------|
| 1. Introduction | 2 |
| 2. Kinks and antikinks in generalized Klein–Gordon equations | 3 |
| 2.1. The model equations | 3 |
| 2.2. Kink dynamics in inhomogeneous media | 3 |
| 2.3. Stability problem | 4 |
| 2.4. Tunnelling | 6 |
| 3. Pair creation and Hawking-like emission | 9 |
| 3.1. Kink–antikink pair creation | 9 |
| 3.2. Hawking-like emission | 11 |
| 4. Discussion | 15 |
| 4.1. Inhomogeneous perturbations | 15 |
| 4.2. Stochastic resonance | 16 |
| 4.3. Solitonic ratchets | 16 |
| 4.4. Hawking emission in Josephson junctions | 17 |
| 4.5. Domain wall tunnelling | 18 |
| 5. Conclusion | 18 |
| Acknowledgments | 18 |
| References | 19 |

1. Introduction

Escape from a metastable state of a dynamical system is of near universal importance. It plays a crucial role in many classes of physical phenomena in nonequilibrium systems, including e.g. stochastic resonance, directed diffusion in stochastic ratchets, and nucleation in phase transitions. In the case of a classical point particle, escape over a finite barrier can occur through the action of external perturbations, e.g. noise-assisted barrier crossing [1]–[3]. A quantum particle can leave the well by tunnelling through the classically forbidden region, and this is true even for macroscopic quantum objects [4]. There have been great advances in the understanding of macroscopic quantum tunnelling, including the quantum mechanics and tunnelling of vortices, domain walls and fluxons [5]–[10].

In cosmology and particle physics, there is an additional way for a particle to escape from a potential well: through the so-called Hawking radiation. Classically, the gravitation is so powerful around a black hole that nothing, not even radiation, can escape from it. Hawking has shown, however, that quantum effects allow black holes to emit radiation. A simplified view of this process is that vacuum fluctuations cause a particle–antiparticle pair to appear close to the event horizon. One particle of the pair falls into the black hole, while the other escapes. To an outside observer it appears that the black hole has emitted a particle [11, 12].

In the present paper, we extend these ideas by investigating the mechanisms by which a (classical) kink soliton can escape from a potential well created by space-dependent external perturbations.

The paper is organized as follows: in section 2, we review well-known results about the kink solutions in nonlinear Klein–Gordon equations, the model equations and kink dynamics in inhomogeneous media. For the presentation of the new phenomena, it is very important

to understand that inhomogeneous media can create potential wells and barriers for the kink motion.

The main result of the paper is discussed in section 3: the Hawking-like emission of a kink from a potential well. In section 3.1, we review the stability and instabilities of the kink modes, as these are crucial for understanding of the main result presented in section 3.2.

In section 4, we discuss some implications of the results in a wider context and the possible ways of observing the new phenomena in real experiments. The phenomena of stochastic resonance and ratchet motion are well known, and are described briefly in sections 4.2 and 4.3. However, some of the implications of our results are discussed here for the first time, e.g. a new kind of solitonic ratchet based on the Hawking-like kink escape in section 4.3. The possibility that the Hawking-like emission process might be observable in long Josephson junctions and domain wall dynamics is considered in sections 4.4 and 4.5.

2. Kinks and antikinks in generalized Klein–Gordon equations

2.1. The model equations

As a model system, we take a nonlinear Klein–Gordon equation:

$$\phi_{tt} - \phi_{xx} + \frac{\partial U(\phi)}{\partial \phi} = F(x), \quad (1)$$

where $U(\phi)$ is a potential that possesses at least two minima. The sine-Gordon and ϕ^4 equations are particular examples of (1) [13]–[15].

The Klein–Gordon equation (1) can be derived from the Lagrangian

$$\mathcal{L} = \frac{1}{2}\phi_t^2 - \frac{1}{2}\phi_x^2 - U(\phi) + F(x)\phi + k.$$

If we define the momentum $\Pi = \frac{\partial \mathcal{L}}{\partial \phi_t}$, then the associated Hamiltonian will be

$$\mathcal{H} = \frac{1}{2}\Pi^2 + \frac{1}{2}\phi_x^2 + U(\phi) - F(x)\phi - k,$$

where $\frac{dk}{dt} = 0$. The energy conservation law can be written as $\frac{dH}{dt} = 0$, where $H = \int_{-\infty}^{\infty} \mathcal{H} dx$.

Equation (1) is a paradigmatic model that supports kink and antikink solutions. The importance of kink-solitons arises in part because of their applications, not only to particle physics, but also to diverse phenomena in condensed matter physics, e.g. domain walls in ferromagnets and ferroelectrics, dislocations in crystals, charge density waves, fluxons in long Josephson junctions and Josephson transmission lines [13, 15].

2.2. Kink dynamics in inhomogeneous media

The effective potential $V(x)$ for the kink is created by the external force $F(x)$, and not by the nonlinearity in ϕ [15]–[23]. However, the nonlinearity in ϕ that corresponds to potential $U(\phi)$ is necessary for the existence of the kink. Suppose $U(\phi)$ possesses three extrema ϕ_1 , ϕ_2 and ϕ_3 , where ϕ_1 and ϕ_3 are minima and ϕ_2 is a maximum. Once $U(\phi_1) = U(\phi_3)$, the kink behaves as a free particle governed by Newton's first law.

The exact solution for the ϕ^4 kink, $\phi_k = \tanh \left[\frac{x-vt-x_0}{2\sqrt{1-v^2}} \right]$, is well known and shows clearly that we cannot consider $U(\phi)$ as the potential in which the kink is moving. The differences

between the bistability in $U(\phi)$ and $V(x)$ have been discussed in connection with soliton stochastic resonance [20]. The fact that $U(\phi)$ should in general have at least two minima for the existence of kinks is discussed in [21]. The case when $F(x) = \text{const} \neq 0$ that leads to $U(\phi_1) \neq U(\phi_3)$ is discussed in [21, 22].

It is well known [22] that when $F(x) = \text{const} < 0$, the kink will move to the right (positive x -direction) and when $F(x) = \text{const} > 0$, the kink will move to the left. This behaviour depends on the sign of the topological charge, so that for the antikink we have the opposite movements. In general, if $F(x)$ has a zero (say at $x = x_*$) and $F(x) \rightarrow F_2 > 0$ for $x \rightarrow \infty$ and $F(x) \rightarrow F_1 < 0$ for $x \rightarrow -\infty$, this $F(x)$ creates a one-well potential for the kink.

As discussed in [15]–[23] (and references therein), inhomogeneous perturbations of soliton equations, both in the form of external forces or parametric impurities, generate effective potentials of type $V(x_{\text{CM}})$ for the motion of the kink, where x_{CM} is the coordinate of the kink centre of mass. There exist many methods for obtaining this effective potential.

An appropriate expression for the effective force that acts on the kink, in terms of the centre of mass of the kink x_{CM} , is

$$F(x_{\text{CM}}) = -2 \int_{-\infty}^{\infty} F(x) f_0(x - x_{\text{CM}}) dx, \quad (2)$$

where $f_0(x)$ is the translational mode. The effective potential satisfies the equation

$$F(x_{\text{CM}}) = -\frac{\partial V(x_{\text{CM}})}{\partial x_{\text{CM}}}. \quad (3)$$

In the case of ϕ^4 -equation,

$$f_0(x) = \text{sech}^2\left(\frac{x}{2}\right). \quad (4)$$

For the antikink equation (2) should be multiplied by (-1) . There are exact solutions for the case where $F(x)$ is not constant [22]. For instance, for

$$F(x) = B(4B^2 - 1) \tanh(Bx), \quad (5)$$

the exact kink solution is $\phi_k = 2B \tanh(Bx)$.

In fact, what is important about equation (5) is that there exists a zero for $F(x)$. In this case, for $4B^2 > 1$ the force (5) gives rise to a stable equilibrium for the kink centre of mass. Both theoretical and numerical investigations show that perturbations of the initial position of the kink centre of mass lead to oscillations of this variable around the point $x = 0$.

2.3. Stability problem

There are two important techniques for investigation of kink dynamics in the presence of perturbations. One is the collective coordinate approach [17, 18] and the other is stability analysis. Sometimes they complement each other.

The main objective of this subsection is to explain the stability conditions for the kink in the presence of an inhomogeneous $F(x)$ with a zero x_* such that $(F(x_*) = 0)$. In this subsection, we will use both techniques to explain the stability conditions because both approaches can shed light on the problem. One example of the application of the collective coordinate approach is to use the ansatz $\phi = \phi_k[x - x_{\text{CM}}(t)]$. The key idea of the technique is to derive a dynamical equation for the collective coordinate $x_{\text{CM}}(t)$ that describes the dynamics of the kink centre of

mass. In [15]–[17], [23], several ways for obtaining this dynamical equation are discussed. The effective force given by (2) is a result of such a technique.

We now present the stability problem. We consider perturbations of a kink-soliton placed at an equilibrium position created by the force $F(x)$. This analysis leads to the spectral problem

$$\hat{L}f = \Gamma f, \quad (6)$$

where $\phi(x, t) = \phi_k(x) + f(x)e^{\lambda t}$,

$$\hat{L} = -\partial_x^2 + \left\{ \frac{\partial^2 U}{\partial \phi^2} \Big|_{\phi=\phi_k} \right\}, \quad \Gamma = -\lambda^2. \quad (7)$$

There are discrete eigenvalues corresponding to soliton modes (a translational mode Γ_0 , internal modes Γ_i , and a continuous spectrum corresponding to phonon modes). Many interesting phenomena can be uncovered by solving this eigenvalue problem for different forms of the function $F(x)$.

Let us discuss the stability conditions when $F(x)$ possesses only one zero, say at x_* , such that $\frac{\partial F(x)}{\partial x} \Big|_{x=x_*} > 0$. We then find that the point $x = x_*$ is a stable equilibrium position for the kink. Otherwise, if $\frac{\partial F(x)}{\partial x} \Big|_{x=x_*} < 0$, the equilibrium position $x = x_*$ is unstable. An easier way to explain this is as follows: from equation (2) we get that for intervals where $F(x) > 0$, the kink will be pushed to the left, whereas for intervals where $F(x) < 0$, the kink will be pushed to the right. Thus if $x = x_*$ is a zero of $F(x)$ and $F(x) < 0$ for $x < x_*$ and $F(x) > 0$ for $x > x_*$, then $x = x_*$ is a stable equilibrium position.

We should add that other exact solutions for a kink moving in the presence of an external force [22] corroborate the result that the sign of $F(x)$ defines the direction of kink motion, and that the points x_* where $F(x)$ changes its sign correspond approximately to the equilibrium positions with $\frac{\partial F(x)}{\partial x} \Big|_{x=x_*} > 0$ as the stability condition. The stability condition for the antikink is $\frac{\partial F}{\partial x} \Big|_{x=x_*} < 0$.

As an illustration of the application of the stability analysis, consider the following inhomogeneous force $F(x) = B(4B^2 - 1) \tanh(Bx)$. It has only one zero $x = 0$. The kink solution is $\phi_k = 2B \tanh(Bx)$.

The operator \hat{L} in the spectral problem (6) does not explicitly depend on $F(x)$. However, it contains information on $F(x)$ because it depends on $\phi_k(x)$; and $\phi_k(x)$ depends on $F(x)$. The calculation of the eigenvalues of \hat{L} for this $F(x)$ and $\phi_k(x)$ leads to the following stability condition for the translational mode

$$4B^2 > 1. \quad (8)$$

Note that this inequality coincides with the condition $\frac{\partial F(x)}{\partial x} \Big|_{x=x_*} = \frac{B^2(4B^2-1)}{\cosh^2(Bx)} \Big|_{x=0} = B^2(4B^2 - 1) > 0$.

Now suppose that $F(x)$ is qualitatively equivalent to that shown in figure 2. That is, $F(x)$ has a maximum at x_M , a zero at $x = x_*$ and a minimum at x_m . In this case, $\frac{\partial F(x)}{\partial x} \Big|_{x=x_*} < 0$. We have found that if $|F(x_M) - F(x_m)|$ exceeds a critical value, the first internal (shape) mode for the kink becomes unstable ($\Gamma_1 < 0$). The eigenfunction corresponding to this (shape) mode is always equivalent to the function $f_1(x) \sim \frac{\sinh(Bx)}{\cosh^\Lambda(Bx)}$. It is the development of the instability of this mode that leads to the break up of the kink ($\phi_k \sim \tanh(Bx)$) and to the creation of a kink–antikink pair.

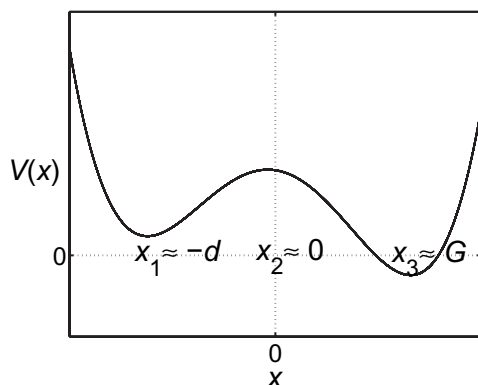


Figure 1. Effective potential for the soliton escape problem modelled with equation (1). As discussed in the text, $V(x)$ is created by the force $F(x)$.

2.4. Tunnelling

We now suppose an external force $F(x)$ such that a point-like kink would feel an effective potential like that shown in figure 1. When the kink-soliton is analysed as a point-like particle (i.e. in terms of collective coordinate theory for its centre of mass [17]), the zeroes of $F(x)$ are equilibrium points [19, 20, 22], [24]–[26]. The effective force acting on the kink centre of mass can be calculated [15, 16]. When the distance between the zeroes of $F(x)$ is comparable with the kink's width, however, the stability conditions for a point particle and an extended kink-soliton clearly differ [19, 20, 22].

For instance, if $F(x)$ possesses three zeroes x_1, x_2, x_3 such that $\frac{\partial F}{\partial x}|_{x_{1,3}} > 0$, $\frac{\partial F}{\partial x}|_{x_2} < 0$ then, for a point-like kink, this would imply the existence of one unstable equilibrium between two stable equilibria. However, if $|x_2 - x_1| < l_k$ and $|x_3 - x_2| < l_k$, where l_k is the kink's width, the point x_2 is no longer unstable for the extended kink-soliton. Thus the kink-soliton will not feel the barrier between the two potential wells.

Gonzalez *et al* [19] investigated the dynamics of a kink moving in an asymmetrical potential well with a finite barrier. For large values of barrier height and thickness, the kink behaves as a point-like classical particle. They also revealed the existence of soliton 'tunnelling' through the potential barrier, a phenomenon linked to stability changes in the presence of many zeroes of the external force [19]. When the kink width is less than those of the well and barrier, the zero x_1 corresponds to a true minimum of the potential: the kink feels the barrier, and it will not move to the right of point $x = x_2$. When the point $x = x_2$ is not unstable, however, the kink can move to the right, crossing the barrier even if its centre of mass is placed in the minimum of the potential and its initial velocity is zero. The kink thus tunnels with sub-barrier kinetic energy [19]. See also the discussion of this phenomenon in the book [16].

We now consider the double-well ϕ^4 potential $U(\phi) = (\phi^2 - 1)^2/8$ and take the force $F(x)$ in the form

$$F(x) = A(4A^2 - 1) \tanh[A(x + d)] \Theta_2(x) + B(4B^2 - 1) \tanh(Bx) \Theta_1(x) \\ + C(4C^2 - 1) \tanh[C(x - G)] \Theta_3(x), \quad (9)$$

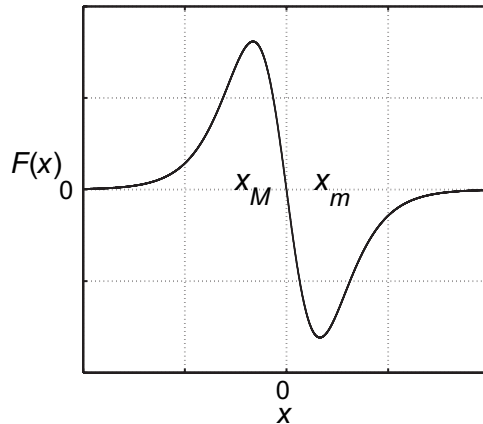


Figure 2. Function $F(x)$ (12) for $4B^2 < 1$.

where

$$\Theta_1(x) = \frac{(\tanh[D(x + (d/2))] + 1)}{2},$$

$$\Theta_2(x) = \frac{(1 - \tanh[D(x + (d/2))])}{2}$$

and

$$\Theta_3(x) = \frac{(\tanh[D(x - (G/2))] + 1)}{2}.$$

The force $F(x)$ is chosen in the form (9) in order to give the three-zero structure discussed above, while allowing for the possibility of exact analytic results. The effective potential for a point-like kink is then equivalent to that shown in figure 1.

The stability problem for the kink solution in the neighbourhood of an equilibrium position can be solved exactly. For $4A^2 > 1$, $4B^2 < 1$, $4C^2 > 1$, $G > d > 0$, the force $F(x)$ corresponds to an effective potential for a point-like kink soliton that possesses a stable equilibrium around $x = x_1 \approx -d$, an unstable equilibrium at $x = x_2 \approx 0$ and a stable equilibrium at $x = x_3 \approx G > 0$. This point corresponds to an equilibrium of lower potential energy than that at $x = x_1 \approx -d$. Figures 3 and 4 show numerical simulations of a kink-soliton when $d = 1$ and $d = 3$, respectively. In all simulations in this paper $D = 4$. The initial conditions used here are

$$\phi(x, t = 0) = \tanh\left[\frac{1}{2}(x + d)\right],$$

$$\phi_i(x, t = 0) = 0.$$

Note that, for $d < 2$ and $\frac{1}{10} < B^2 < \frac{1}{4}$, the kink can tunnel past the barrier despite its initially sub-barrier kinetic energy. However, for $d > 2$, the kink remains trapped in the left potential well. This behaviour can also be seen in figures 5(a) and (b) which show the different dynamical

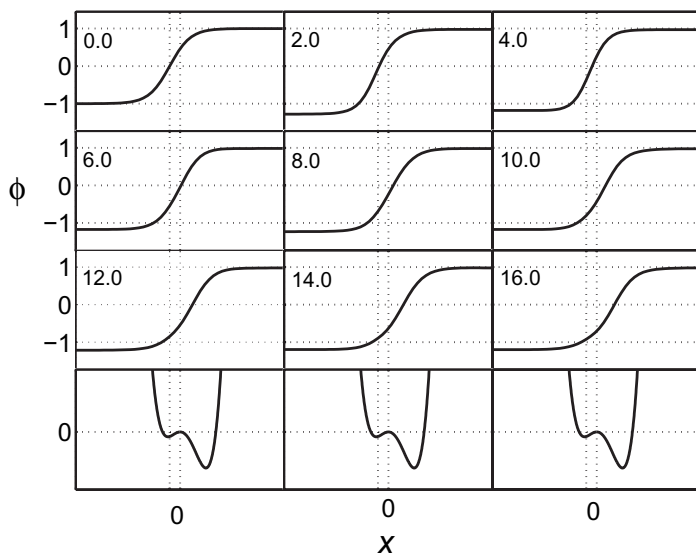


Figure 3. A kink-soliton tunnelling across a potential well. The kink-soliton is initially at $d = 1$ from the origin. The dimensionless time is shown in each frame. The vertical discontinuous lines correspond to the position of the minimum of the potential (left line) and the position of the barrier (right line). The bottom row shows the effective potential in order to make clear the phenomenon.

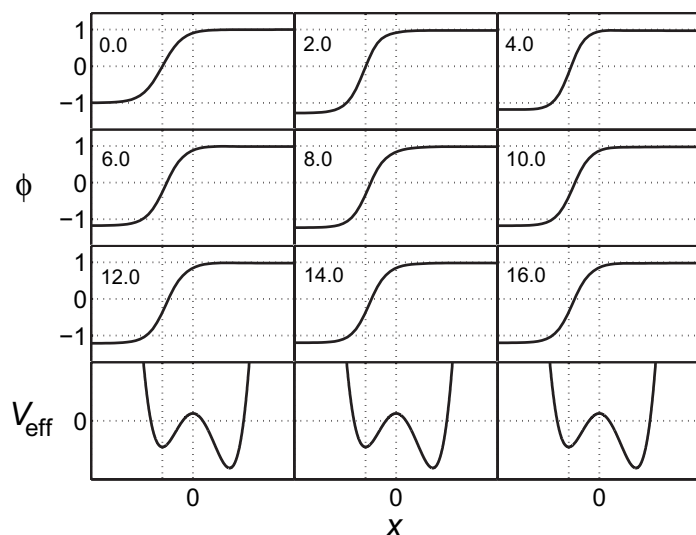


Figure 4. A kink-soliton trapped in a potential well. Initially the kink-soliton is at $d = 3$ from the origin. The dimensionless time is shown in each frame. The vertical discontinuous lines show the position of the minimum (left line) of the potential and the barrier (right line) as in figure 3. The bottom row shows the effective potential in order to make clear the phenomenon.

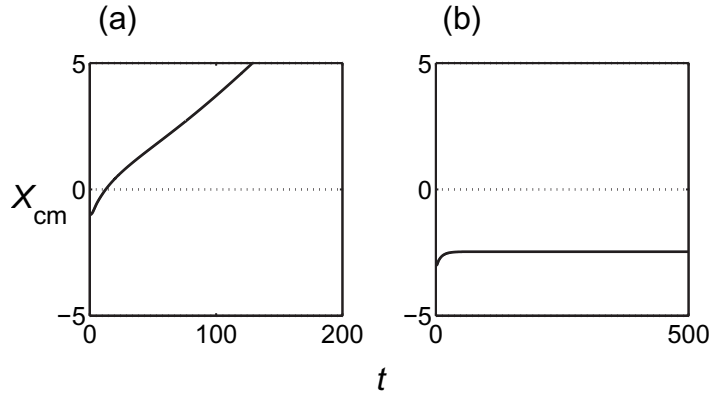


Figure 5. Dynamics of kink-soliton centre of mass in a potential well. (a) Kink-soliton tunnelling across a potential barrier ($d = 1$). (b) Trapped kink-soliton inside the well ($d = 3$).

regimes for the motion dynamics of the kink-soliton centre of mass. Initially, the kink-soliton centre of mass is at the bottom of the potential well created by force $F(x)$ given by (9) (see also figure 1).

We stress that, in the latter situation, the kink behaves very much like a classical particle. To see this, consider thermally activated barrier crossing for

$$\phi_{tt} + \gamma\phi_t - \phi_{xx} + \frac{\partial U(\phi)}{\partial \phi} = F(x) + \eta(x, t). \quad (10)$$

Here $\eta(x, t)$ is a Gaussian white noise with $\langle \eta(x, t) \rangle = 0$ and $\langle \eta(x, t), \eta(x', t') \rangle = 2D\delta(x - x')\delta(t - t')$. The behaviour is then very similar to that in the Kramers model [1].

Furthermore, solitonic stochastic resonance [20] can occur. Consider the equation $\phi_{tt} + \gamma\phi_t - \phi_{xx} + \frac{\partial U(\phi)}{\partial \phi} = F(x) + P_0 \cos(\omega t) + \eta(x, t)$, where $F(x)$ is defined as in (9) with $A = C$, $4A^2 > 1$, $\frac{1}{10} < B^2 < \frac{1}{4}$ and $G = d$. This is equivalent to a symmetric bistable potential for the kink centre of mass. In the absence of noise, the periodic force $P_0 \cos(\omega t)$ is unable to make the kink jump between the wells. It is therefore possible to observe a maximum in a graph of the signal-to-noise ratio (SNR) versus the noise intensity D [20].

3. Pair creation and Hawking-like emission

3.1. Kink–antikink pair creation

As the phenomenon of kink–antikink pair creation is very important for the discussion that follows below, we will dedicate this subsection to its explanation, using a particular example. Let us consider the following equation:

$$\phi_{tt} - \phi_{xx} - \frac{1}{2}\phi + \frac{1}{2}\phi^3 = F(x), \quad (11)$$

where

$$F(x) = \frac{1}{2}(4B^2 - 1) \sinh(Bx) / \cosh^3(Bx). \quad (12)$$

In this case, the exact solution for a static kink placed on the equilibrium point $x = 0$ is $\phi_k = \tanh(Bx)$.

The operator \hat{L} of the spectral problem (6) can be written explicitly in this case:

$$\hat{L} = -\partial_x^2 + \left[1 - \frac{3}{2 \cosh^2(Bx)} \right].$$

This is a Poschl–Teller potential. The eigenvalue problem can be solved exactly [27].

The discrete eigenvalues from the spectral problem (6) are given by the expression $\Gamma_n = -\frac{1}{2} + B^2(\Lambda + 2\Lambda n - n^2)$, where $\Lambda(\Lambda + 1) = 3/2B^2$. The first internal shape mode is unstable when

$$\Gamma_1 < 0. \quad (13)$$

As $\Gamma_1 = B^2(3\Lambda - 1) - \frac{1}{2}$, where $\Lambda = \frac{-1 + \sqrt{1+6/B^2}}{2}$, we obtain the condition for the instability of the first internal shape mode:

$$B^2 < \frac{11 - \sqrt{117}}{8}. \quad (14)$$

The function $F(x)$ has a maximum at certain point $x = x_M$, a zero at point $x = x_* = 0$ (such that $\frac{\partial F}{\partial x}|_{x=x_*} < 0$) and a minimum at certain point $x = x_m$. The condition for the creation of the instability of the first internal (shape) mode can be written in terms of the extrema of the function: $|F(x_M) - F(x_m)| > F_c$, where $F_c = \frac{3}{32}[\sqrt{117} - 9]$. Numerical calculations show that these are good estimates for the critical value F_c even when other functions $F(x)$ (with a maximum, a zero and a minimum) are used. Figure 2 shows the shape of the function $F(x)$ for $4B^2 < 1$. The point $x = 0$ is an unstable equilibrium point for the centre of mass of the kink. The effective potential for $V(x_{CM})$ for the motion of the kink can be defined as follows:

$$V(x_{CM}) = - \int_0^{x_{CM}} F_{\text{ef}}(\xi) d\xi + V_c, \quad (15)$$

where

$$F_{\text{ef}}(\xi) = - \int_{-\infty}^{\infty} (4B^2 - 1) \frac{\sinh(Bx)}{\cosh^3(Bx)} \text{sech}^2\left(\frac{x - \xi}{2}\right) dx, \quad (16)$$

and V_c is an arbitrary constant. Figure 6 shows an illustration of the effective potential $V(x_{CM})$. The effective potential $V(x_{CM})$ can be seen as a potential barrier for the motion of the kink. The effective force is exponentially small everywhere except for a localized zone that contains an unstable equilibrium position that is a maximum of the effective potential. Figure 7 shows the evolution of the instability of the shape mode and the creation of a kink–antikink pair (in addition to the already existing kink).

Thus, if the kink is very close to a potential barrier with these properties, then kink–antikink pairs can be created. This scenario is also valid for any other $F(x)$ with these properties, i.e. it is not restricted to the explicit function used in this simulation. Moreover, the same phenomenon takes place also for the sine-Gordon equation

$$\phi_{tt} - \phi_{xx} + \sin(\phi) = F(x), \quad (17)$$

where $F(x) = 2(B^2 - 1)\sinh(Bx)/\cosh^2(Bx)$. The first internal (shape) mode is unstable for $B^2 < 2/\Lambda_*(\Lambda_* + 1)$, where $\Lambda_* = (5 + \sqrt{17}/2)$. The critical value for $|F(x_M) - F(x_m)|$ is different for the sine-Gordon, but the shape of $F(x)$ is similar to that in equation (12).

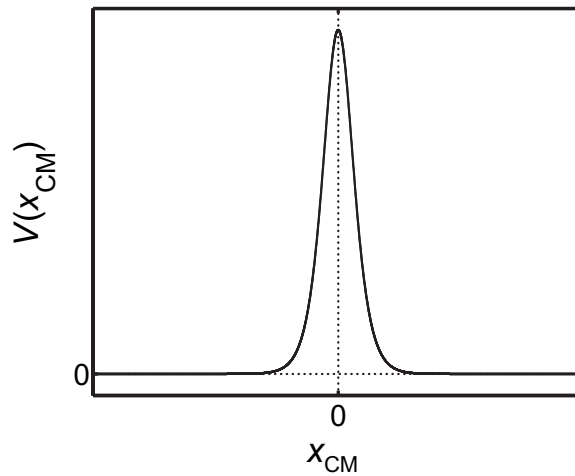


Figure 6. Effective potential barrier $V(x_{CM})$ created by the force (12).

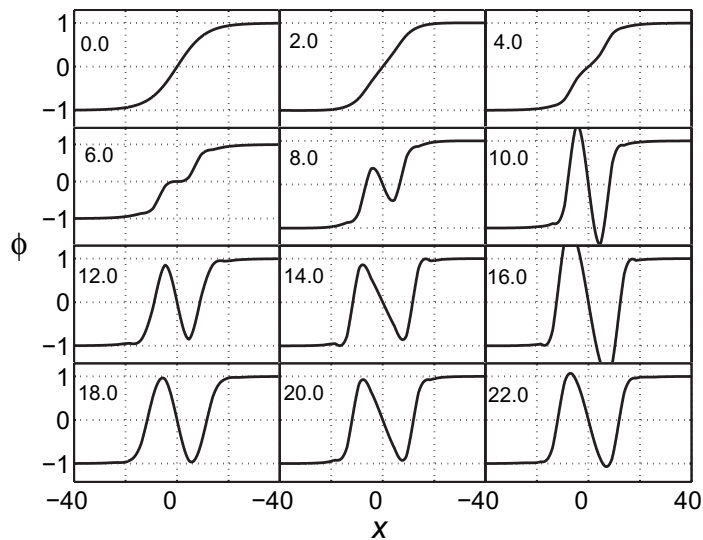


Figure 7. Kink–antikink pair creation via the internal mode instability. The dimensionless time is shown in each frame.

3.2. Hawking-like emission

We now show that a kink can be emitted from the potential well via an internal mode instability, even when the height and thickness of the barrier are very large. A kink–antikink pair can be created near the potential barrier due to the internal mode instability of the original kink. The antikink will be attracted by the potential barrier (a stable equilibrium for the antikink), and the kink then escapes in a process resembling Hawking emission.

Let us consider the situation where $G > d > 2$, such that kink tunnelling is impossible, but where the absolute value of the derivative of $F(x)$ at the point $x = 0$ is such that new instabilities can develop. Thus the equilibrium points are sufficiently separated but $\left| \frac{\partial F(x)}{\partial x} \right|_{x=0}$ can take relatively large values. A stability analysis [22] considering perturbations around a kink-soliton placed at the equilibrium position $x = 0$ [$\phi(x, t) = \phi k(x) + f(x)e^{\lambda t}$] leads to the

eigenvalue problem

$$\hat{L}f = \Gamma f, \quad (18)$$

where $\hat{L} = -\partial_x^2 + \left(6B^2 - \frac{1}{2} - \left(\frac{6B^2}{\cosh^2(Bx)}\right)\right)$, $\Gamma = -\lambda^2$. There are both discrete and continuous spectra. The discrete eigenvalues correspond to soliton modes: a translational mode Γ_0 and an internal mode Γ_1 . The continuous spectrum (Γ_k , $k > 1$) corresponds to phonon modes [22]. In the present case,

$$\Gamma_0 = 2B^2 - \frac{1}{2} \quad \text{and} \quad \Gamma_1 = 5B^2 - \frac{1}{2}. \quad (19)$$

The stability condition for the equilibrium point $x = 0$ of the kink is defined by the eigenvalue of the translational mode [$f_0(x) = (1/\cosh^2(Bx))$], i.e. $4B^2 > 1$. When the kink equilibrium position $x = 0$ is unstable (i.e. $4B^2 < 1$), but $10B^2 > 1$, the kink can move away from the point $x = 0$ without large deformations. The reason is that the internal (shape) mode $f_1(x) = (\sinh(Bx))/(\cosh^2(Bx))$ is still stable.

For $10B^2 < 1$, however, the internal mode becomes unstable, leading to decay of the kink into an antikink and two kinks (see figure 9). For a kink equilibrated on a single barrier like $F(x) = B(4B^2 - 1) \tanh(Bx)$ such that the internal mode is unstable, the initial stage of kink deformation is described by the solution

$$\phi(x, t) = \tanh\left(\frac{x}{2}\right) - f_{1_0} \frac{\sinh(Bx)}{\cosh^2(Bx)} e^{\lambda t}.$$

Note that, even if the initial perturbation of the kink shape is very small ($f_{1_0} \ll 1$), the slope of $\phi(x)$ at its centre of mass will eventually be negative, so that the kink will break up, producing an additional kink–antikink pair. Note also that the amplitude of the deformation cannot increase indefinitely because of energy conservation. In fact, the final state is an antikink at point $x = 0$, and two kinks moving in opposite directions (where $\phi(x, t)$ is finite everywhere).

The whole dynamics of the kink–antikink pair creation and the kink escape in the two-well potential produced by $F(x)$ defined as in (9) can be described using the dynamics of the kink and antikink configurations, the translational mode and the internal (shape) mode [22, 23]. It can be proved that there exists a stable equilibrium stationary solution (see figure 8) that corresponds approximately to the final state that is represented in figure 9.

We have constructed a solution that describes this stable stationary state:

$$\phi_f(x) = 2A \tanh[A(x+d)]\Theta_2(x) + 2C \tanh[C(x-G)]\Theta_3(x) - f_1 \tanh[Qx]\Theta_1(x)\Theta_4(x), \quad (20)$$

where $\Theta_4(x) = \frac{1 - \tanh[D(x-(G/2))]}{2}$, $Q = B$ and $f_1 = 2C$.

The energy balance equation is satisfied approximately H (initial conditions) = H (final state). We should recall that the perturbed Klein–Gordon equation (1) is not completely integrable and part of the energy is radiated in the form of ‘phonon’ waves. That is, the whole energy H is conserved, but not all the energy is solitonic for $t \rightarrow \infty$.

Due to the properties of functions $\Theta_i(x)$, which for $D \gg 1$ behave as Heaviside functions, the stability problem of solution (20) can be reduced to three simpler spectral problems similar to that formulated in equation (18). The solution is stable for $4A^2 > 1$, $4B^2 < 1$, $4C^2 > 1$.

A more physically motivated explanation of the process may also be useful. The initial condition is a kink placed close to the point $x = 0$. Due to the conditions discussed above, the internal mode of this kink is unstable, leading to the creation of a kink–antikink–kink structure. After that, the first kink will be placed on the left side of the point $x = 0$ (the barrier). Here,

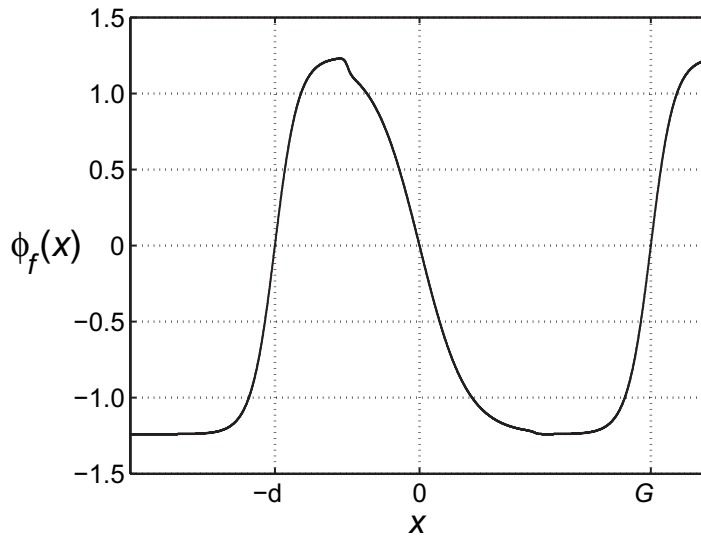


Figure 8. When the internal mode of the kink near the barrier is unstable, the stable stationary field configuration is a kink (inside the left well), an antikink (near the barrier), and a kink that has escaped to the right well.

the function $F(x)$ as defined by equation (9) is positive. So this kink will effectively be pushed to the left and it will be finally captured by the zero of function $F(x)$ near $x = -d$. This is a stable equilibrium for the kink. The antikink will be close to the point $x = 0$. As $\frac{\partial F}{\partial x}|_{x=0} < 0$, this is a stable equilibrium for the antikink. So the antikink remains close to this point. The ‘third particle’ of the trio (the other kink) will be placed on the right side of point $x = 0$, where function $F(x)$ as defined by equation (9) is negative. Thus, this kink will be pushed to the right until it is finally captured by the equilibrium situated near the point $x = G$.

This scenario leads unambiguously to the Hawking emission of a kink via kink–antikink pair creation. A numerical simulation of this process is shown in figure 9.

The initial conditions in these simulations are $\phi(x, t=0) = \tanh\left[\frac{1}{2}(x+1)\right]$, $\phi_t(x, t=0) = 0$. Effectively, during this process, a kink–antikink pair is created due to the instability of the original kink internal mode. Note that topological charge is conserved. The point $x = 0$ (where $|\frac{\partial F(x)}{\partial x}|_{x=0} < 0$) is an attractive equilibrium position for the antikink. Thus, the potential barrier will capture the antikink, whereas the newly created kink escapes to the right potential well. The original kink remains inside the left potential well (i.e. the kink centre of mass is at a point $x_0 < 0$), but very close to the barrier that is the source of instability.

The emission of a kink-soliton from the potential well by the decay of a kink into an antikink and two kinks can also occur under less strict conditions. Suppose e.g. that the conditions for the internal mode instability are satisfied near the barrier, but that the kink centre of mass is at the bottom of the potential well, i.e. $x_0 = -d$. The kink is an extended object. So even when its centre of mass is at the potential minimum, the kink’s ‘wings’ feel the action of the potential wells. If the values of $[F(x)]$ for $x < -d$ are sufficiently large, the kink is pushed to the right, closer to the barrier, and an instability will develop leading to kink emission as described above. This phenomenon can also be observed in the perturbed sine-Gordon equation, where $U(\phi) = 1 - \cos \phi$. In fact, we can construct a function $F(x)$ that corresponds to a bistable

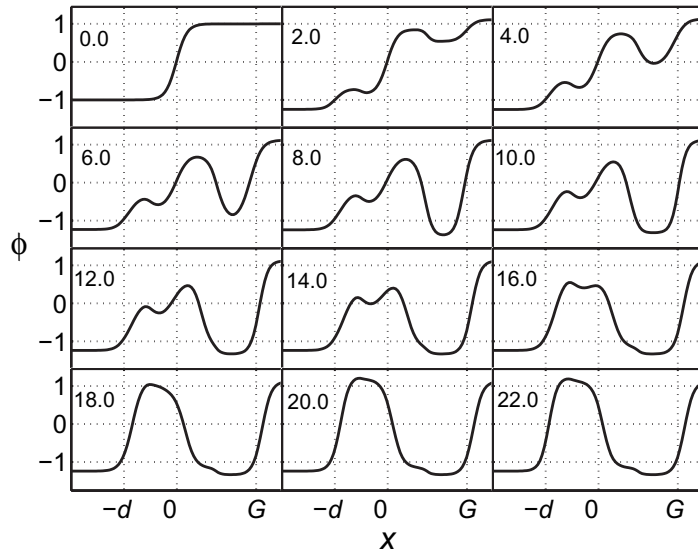


Figure 9. Kink emission via the internal mode instability. The dimensionless time is shown in each frame.

potential for the sine-Gordon kink:

$$F(x) = \frac{2(A^2 - 1)(\sinh[A(x + d)])}{\cosh^2[A(x + d)]} \Theta_2(x) + 2(B^2 - 1)(\sinh[Bx]/\cosh^2[Bx]) \Theta_1(x) + 2(C^2 - 1) \frac{(\sinh[C(x - G)])}{\cosh^2[C(x - G)]} \Theta_3(x), \quad (21)$$

where the $\Theta_i(x)$ functions are defined as in equation (9).

For $B^2 < 2/[\Lambda_*(\Lambda_* + 1)]$, with $\Lambda_* = (5 + \sqrt{17})/2$ the shape mode becomes unstable and the kink–antikink pair is created. We have checked this phenomenon numerically. In general, the relevant features needed for it to occur are the following: $U(\phi)$ should have at least two minima ϕ_1 and ϕ_3 such that for $U(\phi_1) = U(\phi_3)$ the kink can exist (a monotonic function such that $\phi \rightarrow \phi_1$, as $x \rightarrow -\infty$, $\phi \rightarrow \phi_3$ as $x \rightarrow \infty$); and $F(x)$ should generate a barrier such that the first internal shape mode is unstable. The shapes of the kink and the internal mode are very similar in all equations of type (1). In the case of sine-Gordon, the exact kink solution of the unperturbed equation is $\phi_k(x, t) = 4 \arctan\{\exp[(x - vt - x_0)/\sqrt{1 - v^2}]\}$.

Now, returning to the ϕ^4 -equation, if $F(x)$ is such that $|F(x_M) - F(x_m)| > F_c$, the barrier can create a kink–antikink pair even if the original kink is very far inside the potential well (see figure 10). Here, the initial conditions are $\phi(x, t = 0) = \tanh[\frac{1}{2}(x + 10)]$, $\phi_t(x, t = 0) = 0$. Figures 5, 9 and 10 are the results of numerical simulations of the partial differential equation (1). We have used a standard implicit finite difference method with open boundary conditions $\phi_x(-l, t) = \phi_x(l, t) = 0$ and a system length $2l = 2000$. However, the phenomena described do not depend on the numerical method. In the simulations shown in figures 9 and 10, the initial conditions used were the exact stationary kink solutions of the unperturbed ϕ^4 -equation: $\phi_k = \tanh[\frac{x - x_0}{2}]$, where x_0 defines the initial position of the kink centre of mass. If we use different functions as initial conditions, but with a kink-like shape and the same topological charge, the initial deformations in the time evolution of the field $\phi(k, t)$ will of

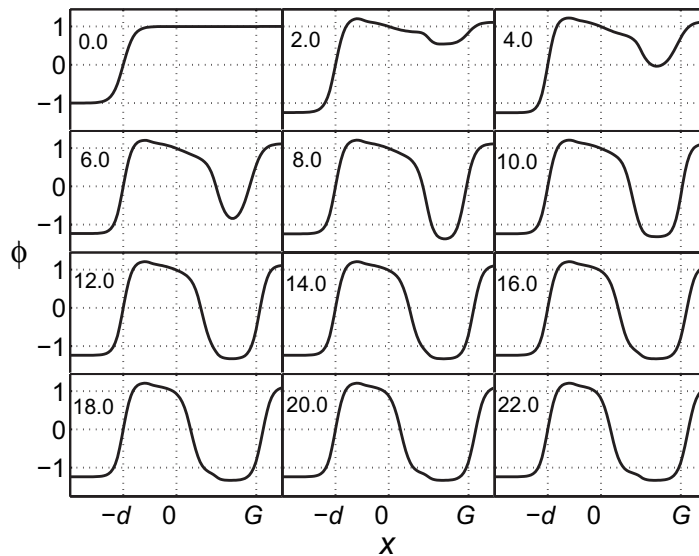


Figure 10. A kink–antikink pair is created outside the potential well barrier even when the initial kink is very deep inside the well. The antikink is attracted to the barrier and the kink escapes to the right potential well. The dimensionless time is shown in each frame.

course differ. However, the main qualitative features of the described phenomena will be exactly the same.

All of these phenomena can be perceived as non-local effects attributable to the spatially extended character of the kink. When the kink feels the instability of the barrier, it suffers deformations producing fluctuations in the field $\phi(x, t)$ leading, ultimately, to development of the kink–antikink pair. We remark that these phenomena are robust. They can also occur for other forces $F(x)$ that create three equilibria for the kink, provided that the slope of $F(x)$ at the unstable equilibrium is sufficiently large. Furthermore, $F(x)$ can also be such that there are other equilibria separated from this three-equilibria basic structure.

4. Discussion

We now discuss some properties of the inhomogeneous perturbations used in the present paper. Then we consider applications to stochastic resonance and ratchets, and discuss the possibility that the Hawking-like emission process might be observable in long Josephson junctions.

4.1. Inhomogeneous perturbations

When the centre of mass of a kink is close to the equilibrium position created by $F(x) \sim \tanh(Bx)$, the dynamics of the kink translational mode is equivalent to a harmonic oscillator [20]. Our construction of $F(x)$ in the paper is equivalent to a Kramers model, where a bistable potential with two minima and a maximum is constructed using three parabolas. As already pointed out above, our model is analytically solvable: we can solve the stability problem exactly for both the translational mode and all the internal modes.

Using the geometrical theory of dynamical systems we can extend the results to all models that are topologically equivalent to the present one [20]. This means all the models where (locally) $F(x)$ possesses three zeroes that generate a bistable effective potential for the motion of kink centre of mass can produce this kind of dynamics. Note that the force $F(x)$ does not have to take large values in order to observe these phenomena. For instance, the $F(x)$ given above for the sine-Gordon equation has the property $F(x) \rightarrow 0$ as $x \rightarrow \pm\infty$, and it is small everywhere. This $F(x)$ can also be used for the ϕ^4 equation. The important features are that $F(x)$ should have three zeroes and that, near the central zero, the first internal mode should be unstable.

The case $F(x) = \text{const}$ is very familiar to experimentalists [15]. This is important because the phenomena presented in this paper can be observed using a $F(x)$ constructed with piece-wise-constant forces as follows:

$$\begin{aligned} F(x) &= F_1 < 0, & \text{for } x < x_1 < 0, \\ F(x) &= F_2 > 0, & \text{for } x_1 < x < x_2 = 0, \\ F(x) &= F_3 < 0, & \text{for } x_2 < x < x_3, \\ F(x) &= F_4 > 0, & \text{for } x > x_3, \end{aligned}$$

where $-F_1 = F_4$ and $x_3 > -x_1$. We have a complete theory and simulations. There are some necessary conditions for $\Delta = F_2 - |F_3|$, and for the distance between the equilibrium points (i.e. where $F(x)$ changes sign). Under some conditions, the kink remains trapped inside the left well; under other conditions it can tunnel through the barrier to the right well, or it can escape via a Hawking-like emission.

The piece-wise-constant $F(x)$ could readily be constructed in experiments with domain walls (using e.g. constant external fields) and in long Josephson junctions ([15, 16] and references therein). We comment, firstly, that the $F(x)$ given in these papers is very much like the $F(x)$ described above in the preceding paragraphs. It is almost constant everywhere. However, it has the advantage that it is smooth even though it changes sign three times. Secondly, Hawking-like emission can occur even when the absolute values of $F(x)$ are small everywhere.

4.2. Stochastic resonance

As mentioned above, a kink can [20] be involved in a motion equivalent to the original stochastic resonance paradigm of a particle in a bistable potential [28]. But this is *only* possible when the equilibrium positions of the potential are sufficiently separated such that the kink feels the bistability and the kink internal modes are stable in the neighbourhood of all equilibrium points. Otherwise, the picture shown in the final frames of figures 9 and 10 applies, i.e. an antikink will be stabilized in the central equilibrium positions and each of the wells will be occupied by a kink. We have checked numerically that the time series of the centre of mass of this structure does not then have a maximum in the SNR versus D plot, i.e. stochastic resonance does not occur.

4.3. Solitonic ratchets

These phenomena can also give rise to ratchet behaviour. For the equation $\phi_{tt} + \gamma\phi_t - \phi_{xx} + \left(\frac{\partial U(\phi)}{\partial \phi}\right) = F(x) + \eta(x, t)$, ratchet motion of a single kink is possible provided certain conditions are satisfied by the force $F(x)$ and the noise $\eta(x, t)$. An example is the force

$F(x) = -A\sin(Bx) + 2\mu A\sin(2Bx + \theta)$, where $\mu = \frac{1}{4}$, $\theta = (\pi/2)$. In this case, $\eta(x, t)$ should be coloured noise [29, 30]. Ratchet motion will be affected in cases where the kink does not feel all irregularities of the effective potential, and also by phenomena related to the complex dynamics and stability of kink internal modes. Furthermore, in some cases the kink can be trapped inside the potential well created by $F(x)$ in such a way that the kink translational mode does not exist. In such cases, kink motion is obviously very difficult [19, 23, 24].

The effect discussed in this paper could lead to a new kind of solitonic ratchet in systems where the kink cannot propagate: the kink is trapped in a potential well but, when it is driven by the external perturbation, it approaches the barrier of the potential. A kink–antikink pair is then created, and a kink is emitted. This kink can be trapped in the contiguous well and the process can start again. As a result of this process, kink propagation in one direction is possible even though the original kink has not abandoned its potential well.

4.4. Hawking emission in Josephson junctions

Before considering the possibility of Hawking-like emission in Josephson junctions, we remark that noise-assisted Hawking kink emission is also possible. Consider the case where the properties of $F(x)$ are such that the kink can sit stably at the minimum of the left potential well without being pushed to the barrier by the potential wall, and the values of $F(x)$ near the barrier are such that the kink internal model should be unstable. The presence of noise can then make the kink approach the barrier and break up, producing the same phenomenon as that depicted for the noise-free case in figure 9.

Long Josephson junctions are very good physical objects for the observation of the soliton dynamics. Akoh *et al* [31] constructed a device in which details of the dynamics of individual fluxons could be observed. They created a local inhomogeneity and they were able to capture a fluxon using this inhomogeneity as in a potential well. Then they applied a constant bias current to the system. The effect of all these actions is equivalent to having a kink-soliton inside a potential well with a finite barrier on the (say) right side. They observed the escape of the fluxon from the potential well. The paper in question is not specific about the concepts of soliton tunnelling and soliton Hawking emission, probably because one needs a theoretical framework in order to introduce such concepts. However this experiment could now be repeated using a similar setup, and the Hawking-like emission could be specifically sought.

In order to be definite, we will provide some details about a possible experiment. We consider a device in the form of an NbN–oxide–NbN junction with the dimensions of $2.5 \times 150 \mu\text{m}^2$. A propagating fluxon can be captured at any desired position in the effective potential well created by placing a resistor on the surface of a portion of the long Josephson junction. The surface resistor has a length larger than the Josephson penetration depth λ_J . The NbN film used in the experiment has a London penetration depth λ_L of about 290 nm. Meanwhile λ_J is estimated to be $4 \mu\text{m}$. The dimensions of the surface resistor used to capture the fluxon are $2.5 \times 20 \mu\text{m}^2$. So the length of the resistor should be $20 \mu\text{m}$. The current density J_0 of this Josephson junction is 2 kA cm^{-2} . It is well known that the fluxon dynamics is very well described by the behaviour of kink-solitons [15]. A Josephson pulse generator at the input side of the junction generates a fluxon. A latching current I_r , supplied from a SQUID connected to the resistor can re-drive the captured fluxon. Once a fluxon has been captured in the potential well, a fluxon should be observable on the output side after supplying a current of $I_r = 0.11 \text{ mA}$. This would indicate that the fluxon had escaped from the potential well.

The length of the resistor defines the width of the potential well. We estimate that for resistor lengths of the order of $6\ \mu\text{m}$ and a supply current I_r of the order of $0.1\ \text{mA}$, fluxon tunnelling should be observable. On the other hand, for resistor lengths of the order of $30\ \mu\text{m}$, tunnelling would be impossible. In this latter case, for supply currents of the order of $1\ \text{mA}$ it should be possible to observe an escaping fluxon due to a fluxon–antifluxon pair creation.

The supply current here is proportional to the absolute value of the slope of the potential $V(x)$ in figure 1 for $x < -d$ or, in other terms, to the absolute value of $F(x)$ given by equation (9) for $x < -d$.

4.5. Domain wall tunnelling

Recently, there has been much interest in the macroscopic tunnelling of domain walls [9, 10, 32], e.g. those trapped by crystal defects in a magnet. Usually tunnelling phenomena are studied as purely quantum effects that should occur at very low temperatures. In general, calculations show the probability to be very small [9, 10, 32]. Our results show however that, under the right conditions, escape will occur with certainty.

One experimental manifestation of the macroscopic tunnelling of domain walls is that the rate of the magnetization relaxation processes does not decrease to zero when the temperature is reduced, but maintains a finite value, independent of temperature [3, 7].

The present results suggest that very large domain walls should show not only the macroscopic tunnelling but also the Hawking emission. Other systems with topologically coherent structures, e.g. vortices and spiral waves [33], may be expected to behave similarly. Such phenomena should in principle be observable. In particular, it is in principle possible to build a long Josephson junction, with an inhomogeneous perturbation like the one studied here, where the kink escape could be observed [34]. The perturbation $F(x)$ can be readily implemented through an applied magnetic field to push the domain wall off the defect [10]. This experimental setup has already been used to study ratchets with a moving kink in a medium with potential wells and barriers. Thus, the implementation of the appropriate barrier will not be a problem. The escape of the kink will be reflected in the electrical performance of the junction.

5. Conclusion

We have shown that the Hawking radiation phenomenon is not restricted to the vicinity of black holes, as had been assumed. Rather, it is a more widespread phenomenon that can occur even in condensed matter systems. Our theory of the process is dynamical, and we can follow in detail what happens in simulations. We point to an experiment with a long Josephson junction where we believe that this phenomenon can be observed and where we suspect that it may already have been observed [31], albeit without full appreciation of what was occurring.

Acknowledgments

We acknowledge support of the Engineering and Physical Sciences Research Council (UK). One of us (JAG) is grateful to the Royal Society of London for funding his visit to Lancaster.

References

- [1] Kramers H A 1940 *Physica* **7** 284
- [2] Dykman M I and Krivoglaz M A 1984 *Soviet Physics Reviews* vol 5, ed I M Khalatnikov (New York: Harwood) pp 265–441
- [3] Hanggi P, Talkner P and Borkovec M 1990 *Rev. Mod. Phys.* **62** 251
- [4] Caldeira A O and Leggett A J 1983 *Ann. Phys., NY* **149** 374
- [5] Voss R F and Webb R A 1981 *Phys. Rev. Lett.* **47** 265
- [6] Martinis J M, Devoret M H and Clarke J 1987 *Phys. Rev. B* **35** 4682
- [7] Hendry P C, Lawson N S, McClintock P V E, Williams C D H and Bowley R M 1988 *Phys. Rev. Lett.* **60** 604
- [8] Stamp P C E 1991 *Phys. Rev. Lett.* **66** 2802
- [9] Ao P and Thouless D J 1994 *Phys. Rev. Lett.* **72** 132
- [10] Shnirman A, Ben-Jacob E and Malomed B 1997 *Phys. Rev. B* **56** 14677
- [11] Hawking S W 1975 *Commun. Math. Phys.* **43** 199
- [12] Parikh M and Wilczek F 2000 *Phys. Rev. Lett.* **85** 5042
- [13] Bishop A R, Krumhansl J A and Trullinger S E 1980 *Physica D* **1** 1
- [14] Scott A C 1999 *Nonlinear Science* (Oxford: Oxford University Press)
- [15] Kivshar Yu S and Malomed B A 1989 *Rev. Mod. Phys.* **61** 763
- [16] Braun O M and Kivshar Y S 2004 *The Frenkel–Kontorova Model* (Berlin: Springer)
- [17] Sanchez A and Bishop A R 1998 *SIAM Rev.* **40** 579
- [18] McLaughlin D W and Scott A C 1978 *Phys. Rev. A* **18** 1652
- [19] Gonzalez J A, Bellorin A and Guerrero L E 1999 *Phys. Rev. E* **60** R37
- [20] Gonzalez J A, Mello B A, Reyes L I and Guerrero L E 1998 *Phys. Rev. Lett.* **80** 1361
- [21] Gonzalez J A and Holyst J A 1987 *Phys. Rev. B* **35** 3643
- [22] Gonzalez J A and Holyst J A 1992 *Phys. Rev. B* **45** 10338
- [23] Gonzalez J A, Cuenda S and Sánchez A 2007 *Phys. Rev. E* **75** 036611
- [24] Gonzalez J A, Bellorin A and Guerrero L E 2002 *Phys. Rev. E* **65** 065601
- [25] Gonzalez J A, Guerrero L E and Bellorin A 1996 *Phys. Rev. E* **54** 1265
- [26] Gonzalez J A and Mello B A 1996 *Phys. Lett. A* **219** 226
- [27] Flugge S 1971 *Practical Quantum Mechanics* (Berlin: Springer)
- [28] Dykman M I *et al* 1995 *Nuovo Cimento D* **17** 661
- [29] Reimann P 2002 *Phys. Rep.* **361** 57
- [30] Morales-Molina L *et al* 2006 *Chaos* **16** 013117
- [31] Akoh H, Sakai S, Yasi A and Hayakawa H 1985 *IEEE Trans. Magn.* **21** 737
- [32] Chudnovsky E M, Iglesias O and Stamp P C E 1992 *Phys. Rev. B* **46** 5392
- [33] Cross M C and Hohenberg P C 1993 *Rev. Mod. Phys.* **65** 851
- [34] Beck M *et al* 2005 *Phys. Rev. Lett.* **95** 090603